Supplementary Figure S1

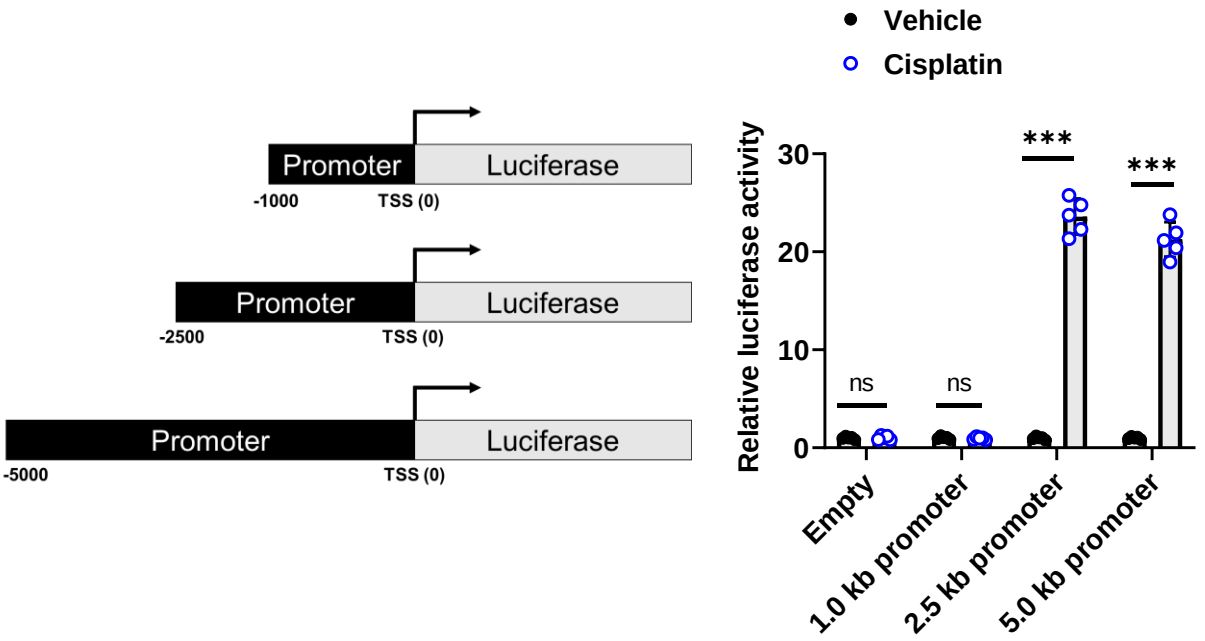

Supplementary Figure S1. ***Development of a promoter assay to examine Sox9 transcriptional regulation***. Murine Sox9 promoter sequences were cloned into a reporter luciferase construct. The left panel shows the three constructs with 1, 2.5, and 5 kb promoter sequences. The promoter-less luciferase (empty) or Sox9-promoter driven luciferase constructs were then transiently transfected into BUMPT cells and 24 hours later treated with vehicle or 25 μM cisplatin for 8 h followed by measurement of luciferase activity. Cisplatin treatment induced a robust induction of luciferase activity that was dependent on the Sox9 promoter. Our results showed that the 2.5 and 5 kb constructs contained the necessary elements for Sox9 transcriptional induction. In the bar graphs (n = 5 biologically independent samples), experimental values are presented as mean ± S.D. The height of error bar = 1 S.D., and $p < 0.05$ was indicated as statistically significant. Student's t test was carried out and statistical significance is indicated by *$P < 0.05$, **$P < 0.01$, ***$P < 0.001$.

Supplementary Figure S2

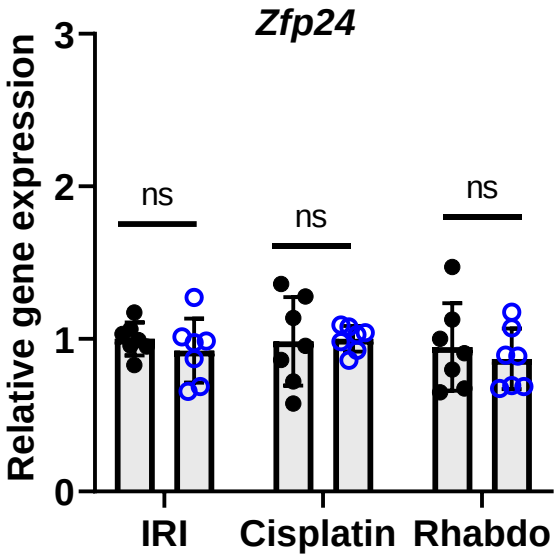

Supplementary Figure S2. ***Renal Zfp24 gene expression during acute kidney injury.*** Ischemia reperfusion (IRI), cisplatin nephrotoxicity, and rhabdomyolysis-associated acute kidney injury was induced in 8–12-week-old male C57BL/6J mice. Bilateral renal ischemia was induced for 30 min, cisplatin nephrotoxicity was induced by a single intraperitoneal cisplatin injection (30 mg/kg), and rhabdomyolysis was induced by glycerol injection (7.5 ml/kg 50% glycerol) in the hind-leg muscles. Sham groups represent either mock surgery or vehicle injections. At 24 h (IRI and rhabdomyolysis) and 72 h (cisplatin) kidney tissues were collected. Gene expression analysis of cortical renal tissues showed that *Zfp24* expression did not change during AKI. In all the bar graphs (n = 7 biologically independent samples from three independent experiments), experimental values are presented as mean ± S.D. The height of error bar = 1 S.D., and $p < 0.05$ was indicated as statistically significant. Student's t test was carried out and statistical significance is indicated by $*P < 0.05$, $**P < 0.01$, $***P < 0.001$.

Supplementary Figure S3

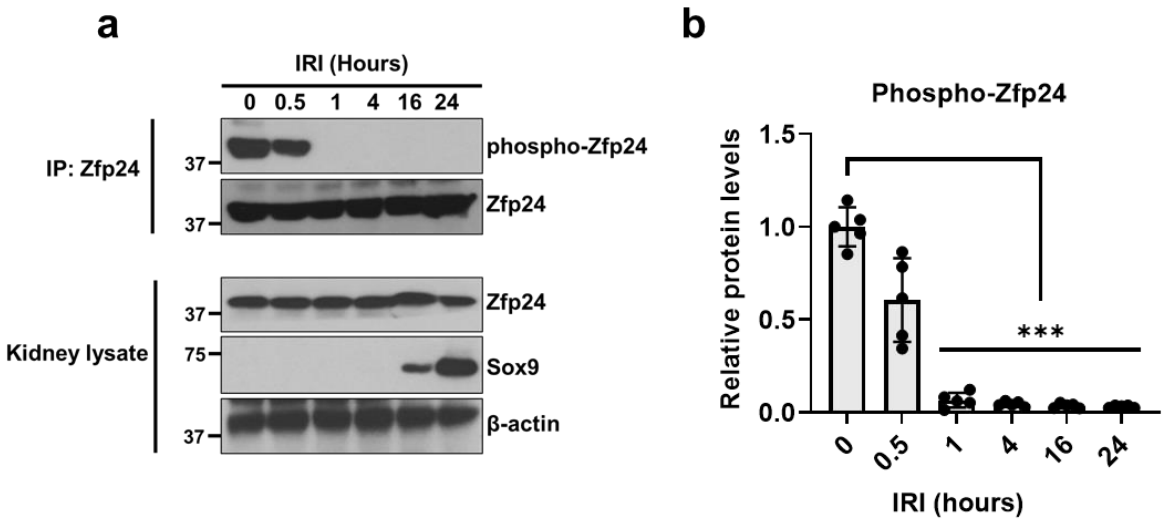

Supplementary Figure S3. ***Zfp24 dephosphorylation is an early event during IRI-associated AKI.*** Bilateral renal ischemia was induced for 30 min, followed by the collection of renal tissues at indicated time points. Renal cortical tissues were used for Zfp24 immunoprecipitation followed by immunoblot analysis of total and phosphorylated Zfp24 using a phospho-linker antibody. Zfp24 was predominantly present in the phosphorylated state at 0 hours followed by de-phosphorylation within 1 hour. (**a-b**) Representative blots show Zfp24 phosphorylation in the renal tissues, while the graph depicts densitometric analysis (Phospho-Zfp24 expression normalized to total Zfp24 levels). In the bar graph (n = 5 biologically independent samples from three independent experiments), experimental values are presented as mean ± S.D. The height of error bar = 1 S.D., and $p < 0.05$ was indicated as statistically significant. One-way ANOVA followed by Tukey's multiple-comparison test was carried out and statistical significance is indicated by by $*P < 0.05$, $**P < 0.01$, $***P < 0.001$.

Supplementary Figure S4

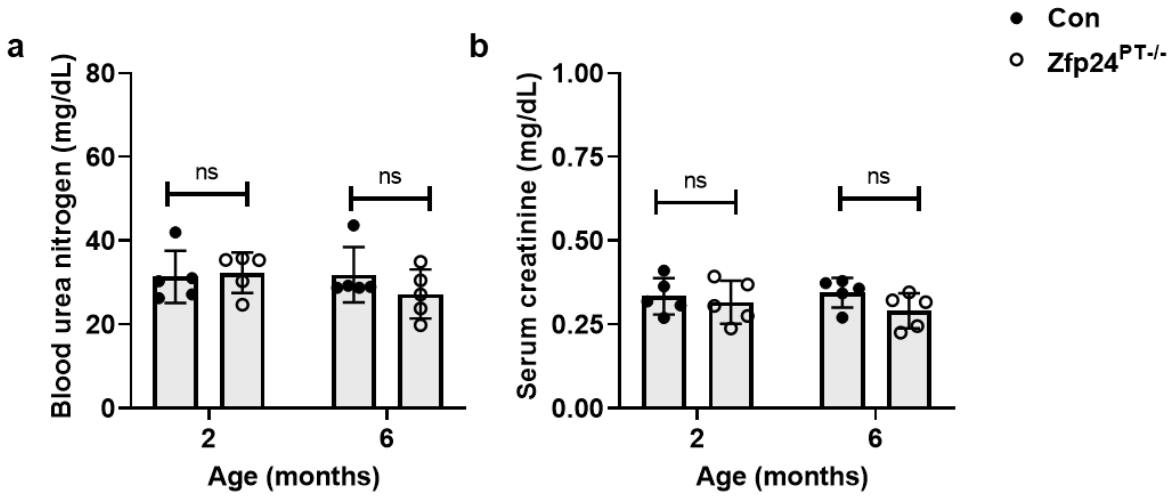

Supplementary Figure S4: ***Effect of Zfp24 gene knockout on kidney function***. Littermate control and Zfp24 conditional knockout mice (indicated by $Zfp24^{PT-/-}$) at 2- and 6-months age had no functional renal impairment as measured by (**a**) Blood urea nitrogen (**b**) Serum Creatinine levels, indicating that Zfp24 gene deletion does not influence renal function under normal baseline conditions. In all the bar graphs (n=5 biologically independent samples), experimental values are presented as mean ± s.d. The height of error bar = 1 s.d. and $p < 0.05$ was indicated as statistically significant. Student's t-test was carried out and statistical significance is indicated by ns=not significant, *$P < 0.05$, **$P < 0.01$, ***$P < 0.001$.

Supplementary Figure S5

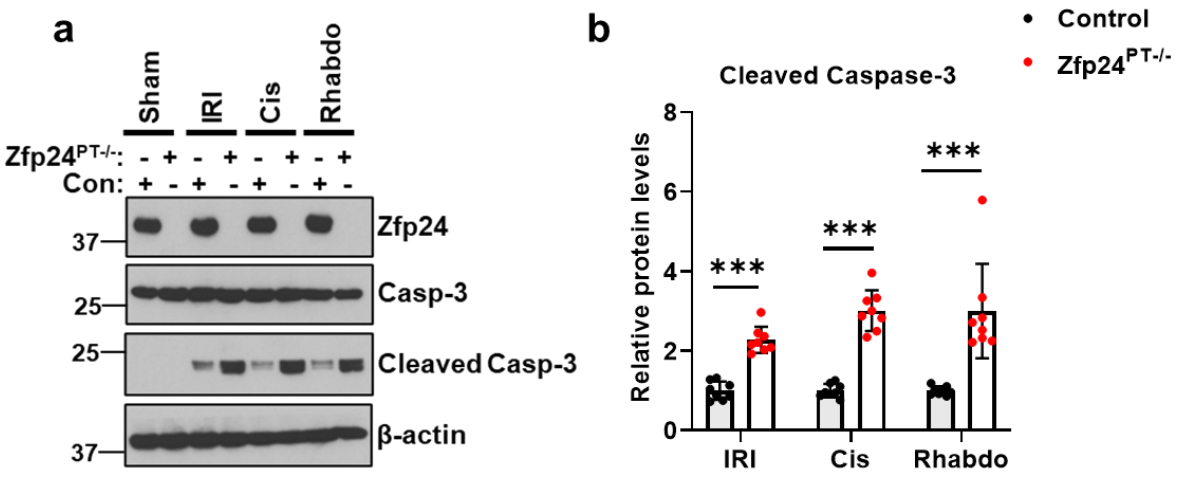

Supplementary Figure S5. ***Zfp24 gene deletion results in increased cell death during AKI.*** Littermate control and Zfp24 conditional knockout mice were challenged with bilateral renal ischemia (30 min), cisplatin (30 mg/kg, single intraperitoneal injection) nephrotoxicity, or glycerol-induced rhabdomyolysis (7.5 ml/kg 50% glycerol in the hind-leg muscles) followed by an examination of caspase-3 activation (cleaved caspase-3) renal tissues. Western blot analysis showed that AKI-induced caspase-3 activation was significantly elevated in the Zfp24 conditional knockout mice. (**a-b**) Blots are representative of four independent experiments. Densitometric analysis was performed for Cleaved Caspase-3 protein expression using Image J and normalization was carried out using β-actin as the loading control. In the bar graph (n = 8 biologically independent samples from 3-4 independent experiments), experimental values are presented as mean ± S.D. The height of error bar = 1 S.D., and $p < 0.05$ was indicated as statistically significant. One-way ANOVA followed by Tukey's multiple-comparison test was carried out, and statistical significance is indicated by $*P < 0.05$, $**P < 0.01$, $***P < 0.001$.

Supplementary Figure S6

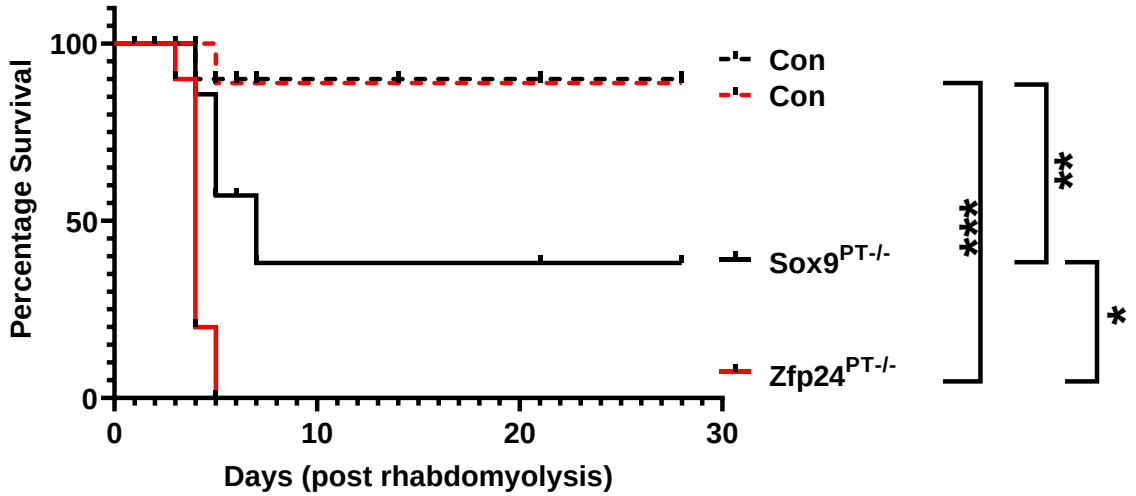

Supplementary Figure S6: ***Zfp24 gene deletion in tubular epithelial cells reduces overall survival from rhabdomyolysis*.** Littermate controls, Zfp24, and Sox9 conditional knockout mice were challenged with glycerol-induced rhabdomyolysis (7.5 ml/kg 50% glycerol in the hind-leg muscles) followed by examination of overall survival up to 4 weeks. While most of the control mice recovered and survived up to 4 weeks, all the $Zfp24^{PT-/-}$ mice died within the first 4 days. The $Sox9^{PT-/-}$ showed intermediate severity as compared to control and $Zfp24^{PT-/-}$ mice. Data is presented as Kaplan-Meier survival curves (n=10 biologically independent samples) and Mantel-Cox test was performed to determine statistical significance.

Supplementary Figure S7

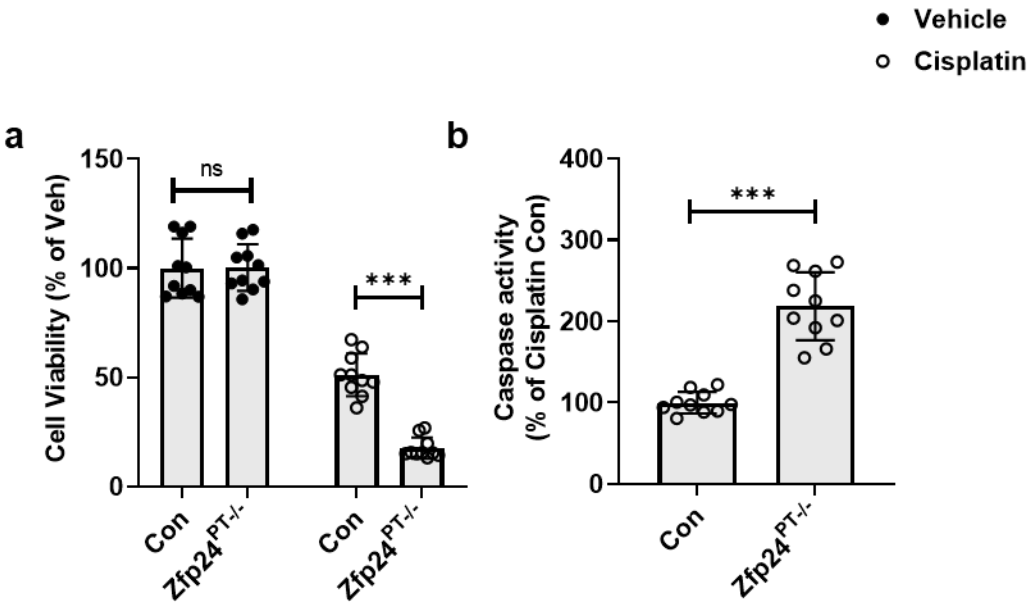

Supplementary Figure S7: ***Zfp24 gene deletion sensitizes primary tubular epithelial cells to cisplatin-induced cell death*.** Primary tubular epithelial cells were isolated from the renal cortex of control and Zfp24 conditional knockout mice followed by treatment with 50 µM Cisplatin for 24 hours. **(a)** Trypan blue based cellular viability and (**b**) caspase activity assay indicate that Zfp24 gene deletion increases the susceptibility to cisplatin-induced cell death. In all the bar graphs (n=10 biologically independent samples), experimental values are presented as mean ± s.d. The height of error bar = 1 s.d. and $p < 0.05$ was indicated as statistically significant. One-way ANOVA followed by Dunnett's was carried out and statistical significance is indicated by *$P < 0.05$, **$P < 0.01$, ***$P < 0.001$.

Supplementary Figure S8

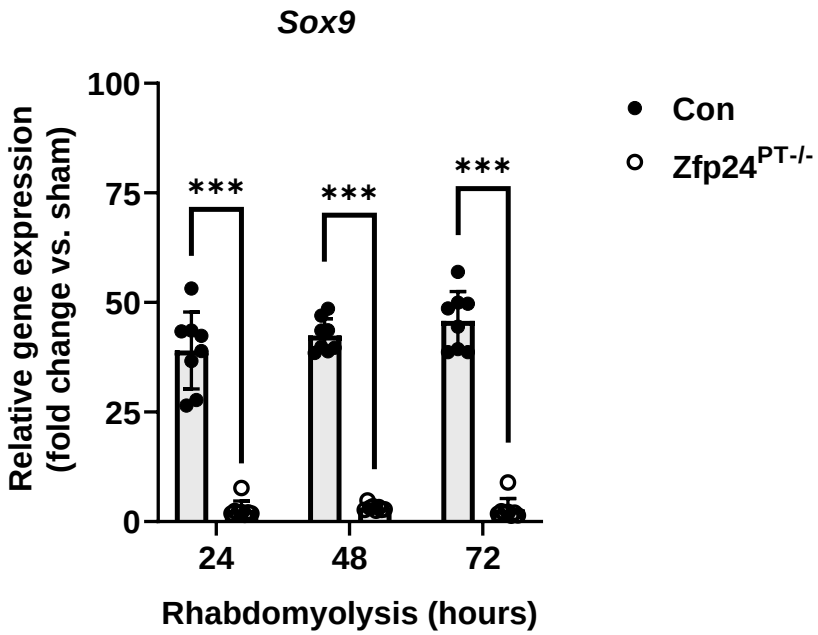

Supplementary Figure S8: ***Time-course analysis of Sox9 gene induction during rhabdomyolysis-associated AKI*.** Littermate control and Zfp24 conditional knockout mice were challenged with glycerol-induced rhabdomyolysis (7.5 ml/kg 50% glycerol in the hind-leg muscles), or sham-treated (vehicle injection) followed by gene expression analysis of Sox9 in renal tissues at indicated time-points. The results show that Zfp24 gene deletion suppresses Sox9 upregulation during AKI. Data are presented as individual data points (n = 8 biologically independent samples), from two independent experiments, all producing similar results. In the bar graph, experimental values are presented as mean ± s.d. The height of error bar=1 s.d. and p<0.05 was considered as statistically significant, while ns indicates not significant. 1-way ANOVA followed by Tukey's multiple-comparisons test was carried out and statistical significance is indicated by **P* < 0.05, ***P* < 0.01, ****P* < 0.001.

Supplementary Figure S9

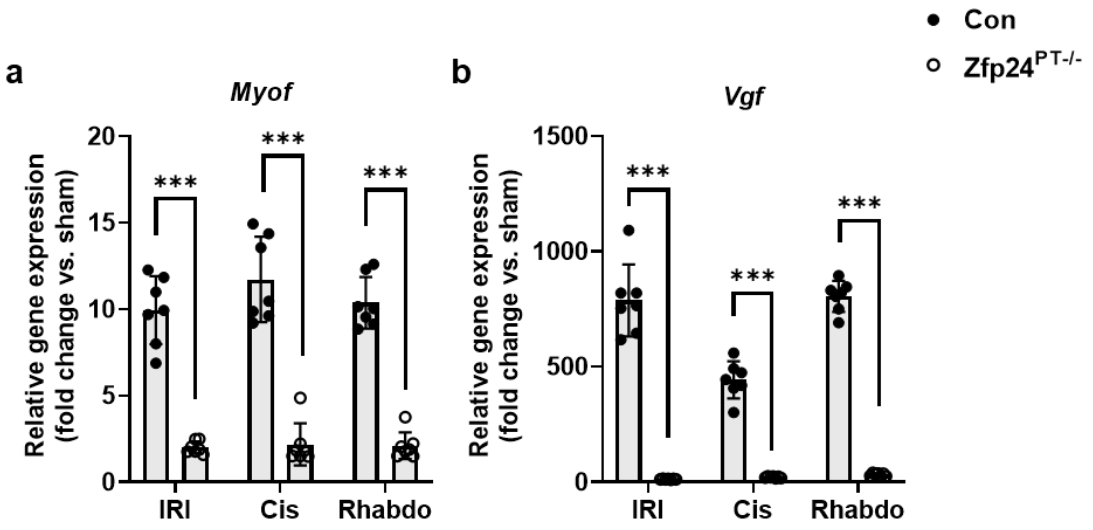

Supplementary Figure S9: ***Expression analysis of Sox9 target genes*.** Littermate control and Zfp24 conditional knockout mice were challenged with bilateral renal ischemia (30 min), cisplatin (30 mg/kg, single intraperitoneal injection) nephrotoxicity, or glycerol-induced rhabdomyolysis (7.5 ml/kg 50% glycerol in the hind-leg muscles) followed by qPCR-based analysis of Sox9 target genes, namely (**a**) Myoferlin and (**b**) VGF nerve growth factor inducible gene. Data are presented as individual data points (n = 7 biologically independent samples), from two independent experiments, all producing similar results. In the bar graph, experimental values are presented as mean ± s.d. The height of error bar=1 s.d. and p<0.05 was considered as statistically significant, while ns indicates not significant. 1-way ANOVA followed by Tukey's multiple-comparisons test was carried out and statistical significance is indicated by by **P* < 0.05, ***P* < 0.01, ****P* < 0.001.

Supplementary Figure S10

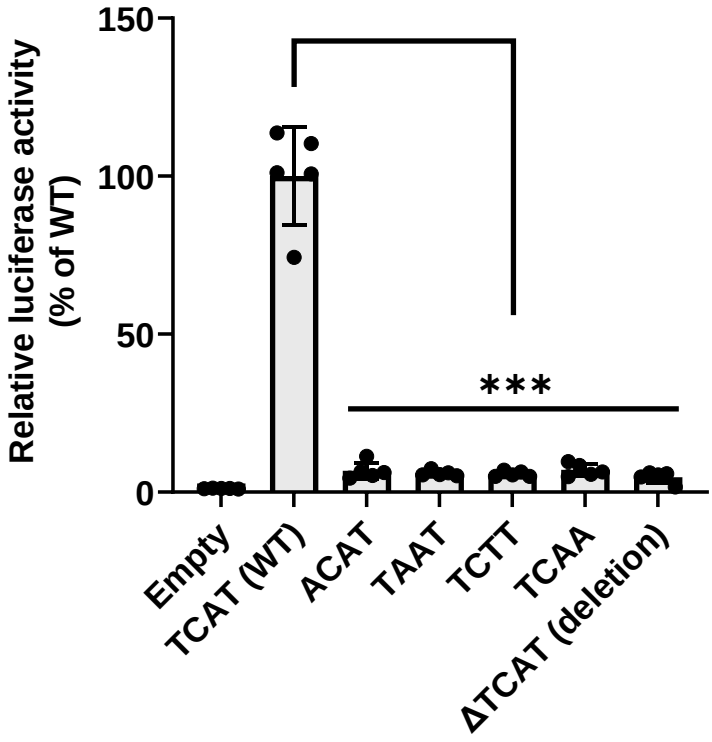

Supplementary Figure S10. ***Functional effect of Zfp24 binding site mutations on Sox9 promoter activation***. Murine Sox9 promoter (0-2500 bp) was cloned into a reporter luciferase construct and named as TCAT (WT) construct. Site-directed mutagenesis was then used to mutate single nucleotides within the TCAT site to generate 4 mutants (ACAT, TAAT, TCTT, and TCAA). A deletion mutant was also generated. The promoter-less luciferase (empty) or WT and mutant luciferase constructs were then transiently transfected into BUMPT cells and 24 hours later treated with vehicle or 25 μM cisplatin for 8 h followed by measurement of luciferase activity. Cisplatin treatment induced a robust induction of luciferase activity in the WT construct but not the mutants. In the bar graphs (n = 5 biologically independent samples), experimental values are presented as mean ± S.D. The height of error bar = 1 S.D., and $p < 0.05$ was indicated as statistically significant. 1-way ANOVA followed by Tukey's multiple-comparisons test was carried out and statistical significance is indicated by $*P < 0.05$, $**P < 0.01$, $***P < 0.001$.

Supplementary Figure S11

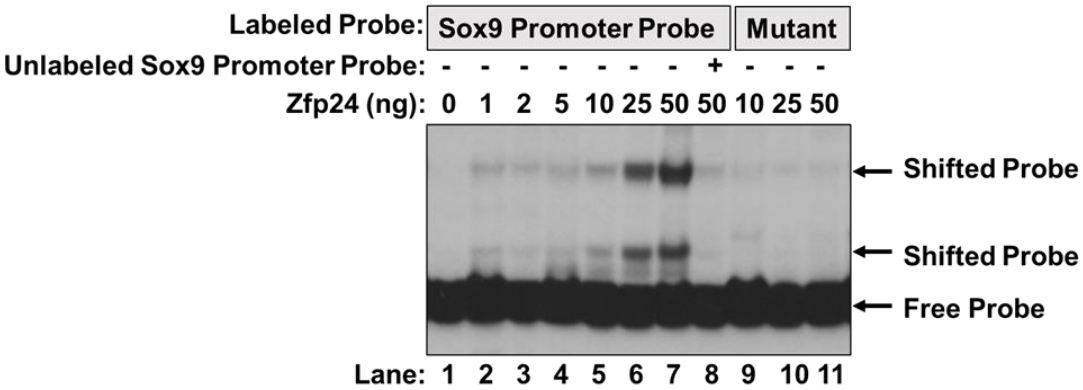

Lane	1	2	3	4	5	6	7	8	9	10	11
Shifted Probe	0	4.2	4.8	6.3	14.8	46.1	100	3.8	2.9	2.7	1.8

Supplementary Figure S11. ***Examination of Zfp24 binding to Sox9 promoter by electrophoresis mobility shift assay (EMSA)***. Biotin 3' end-labeled duplex DNA probe was incubated with purified Zfp24 protein and followed by electrophoresis mobility shift assay. A 50 bp probe surrounding the TCAT sequence in the Sox9 murine promoter was used in the assay (Lane 1-8). As seen in Lane 7, we saw a clear binding of Zfp24 to the labeled probe, which was inhibited by the addition of an unlabeled probe (Lane 8). A mutant labeled probe with TCAT to TAAT mutation was used as a control (Lane 8-11). Zfp24 binding was seen with the TCAT probe (lane 7), which was significantly lower with the TAAT probe (Lane 11). The blot is representative of 3 independent experiments. The table in the lower panel shows the relative intensity (densitometry) of the shifted probe (higher + lower) as compared to Lane 7 (set as 100%).

Supplementary Figure S12

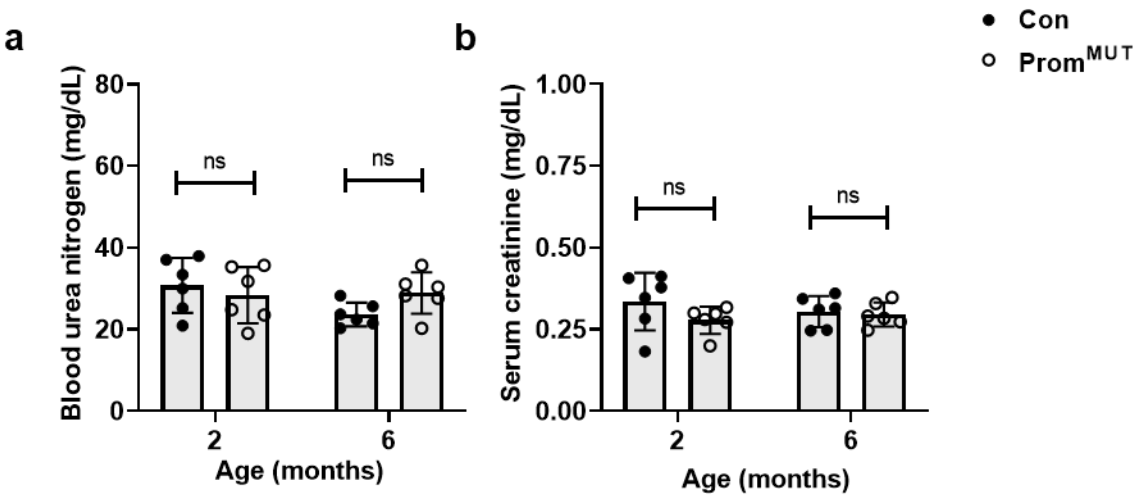

Supplementary Figure S12: ***Effect of Sox9 promoter mutation on baseline kidney function***. Littermate control and knock-in mice with mutation in the Zfp24 binding site in the Sox9 promoter (indicated by $Prom^{mut}$) at 2- and 6-months age had no functional renal impairment as measured by (**a**) Blood urea nitrogen (**b**) Serum Creatinine levels. In all the bar graphs (n=5 biologically independent samples), experimental values are presented as mean ± s.d. The height of error bar = 1 s.d. and $p < 0.05$ was indicated as statistically significant. Student's t-test was carried out and statistical significance is indicated by ns=not significant, **P* < 0.05, ***P* < 0.01, ****P* < 0.001.

Supplementary Figure S13

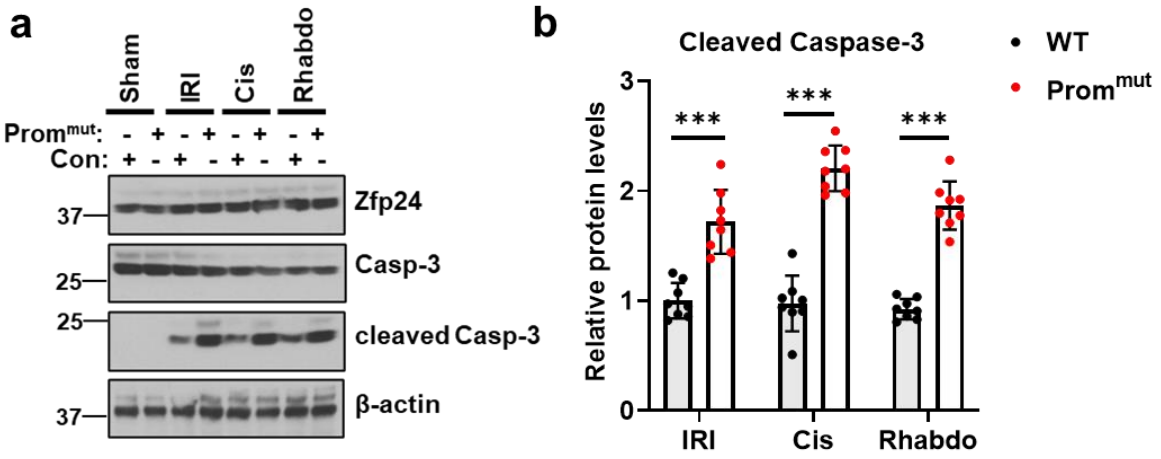

Supplementary Figure S13. ***Prommut mice have increased tubular cell death during AKI.*** Littermate WT and promoter mutant (Prom^{mut}) mice were challenged with bilateral renal ischemia (30 min), cisplatin (30 mg/kg, single intraperitoneal injection) nephrotoxicity, or glycerol-induced rhabdomyolysis (7.5 ml/kg 50% glycerol in the hind-leg muscles) followed by an examination of caspase-3 activation (cleaved caspase-3) renal tissues. Western blot analysis showed that AKI-induced caspase-3 activation was significantly elevated in the Zfp24 conditional knockout mice. (**a-b**) Blots are representative of four independent experiments. Densitometric analysis was performed for Cleaved Caspase-3 protein expression using Image J and normalization was carried out using β-actin as the loading control. In the bar graph (n = 8 biologically independent samples from 3-4 independent experiments), experimental values are presented as mean ± S.D. The height of error bar = 1 S.D., and $p < 0.05$ was indicated as statistically significant. One-way ANOVA followed by Tukey's multiple-comparison test was carried out, and statistical significance is indicated by $*P < 0.05$, $**P < 0.01$, $***P < 0.001$.

Supplementary Figure S14

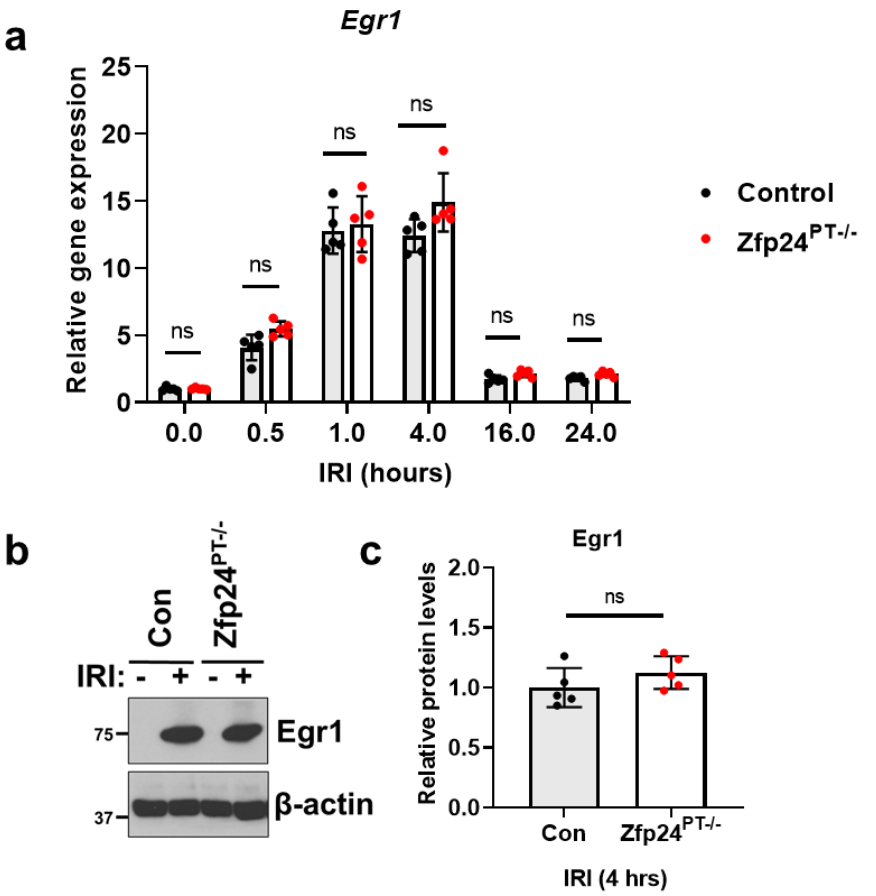

Supplementary Figure S14. ***Egr1 expression is not altered in Zfp24 conditional knockout mice.*** Bilateral renal ischemia was induced for 30 min in the littermate control and Zfp24 conditional knockout mice, followed by the collection of renal tissues at indicated time points. (**a**) Gene expression analysis showed that AKI-induced Egr1 upregulation is not affected by Zfp24 gene deletion (**b-c**) Immunoblot analysis showed that Zfp24 protein levels were similarly induced in the kidneys of control and Zfp24 conditional knockout mice at 4 hours post-IRI. Blots are representative of two independent experiments, while the graph depicts densitometric analysis (Egr1 expression normalized to total β-actin levels). In the bar graph (n = 5 biologically independent samples from three independent experiments), experimental values are presented as mean ± S.D. The height of error bar = 1 S.D., and $p < 0.05$ was indicated as statistically significant. Student's t test was carried out and statistical significance is indicated by $*P < 0.05$, $**P < 0.01$, $***P < 0.001$.

Supplementary Figure S15

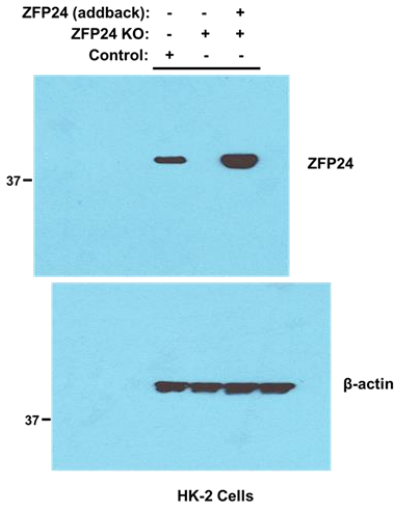

Figure 1f

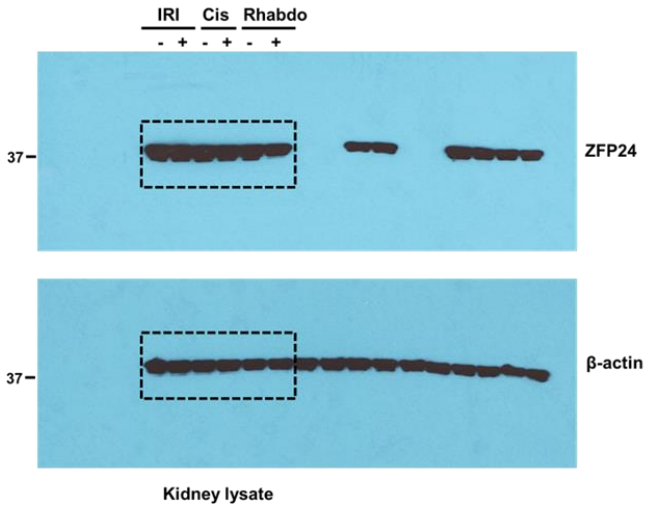

Figure 2c

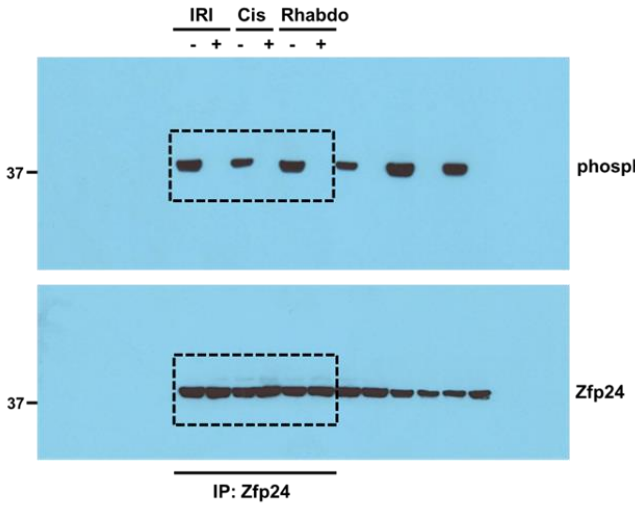

Figure 2e

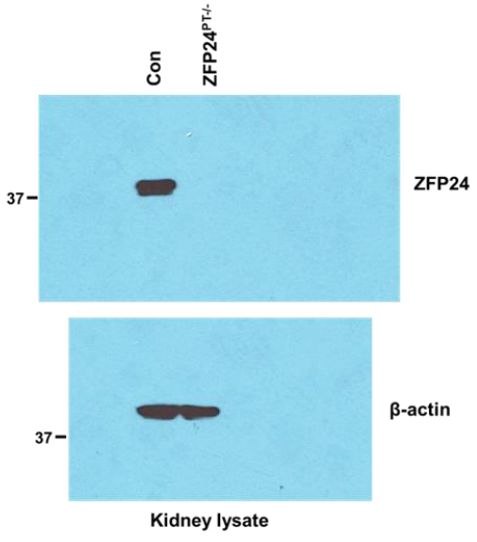

Figure 3a

Suppl. Figure S15: ***Uncropped images of immunoblot data.***

Supplementary Figure S15 (continued)

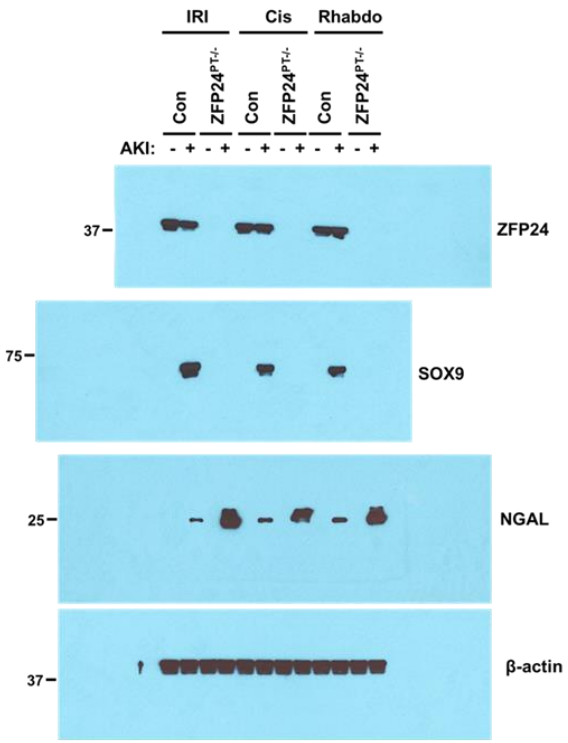

Figure 4c

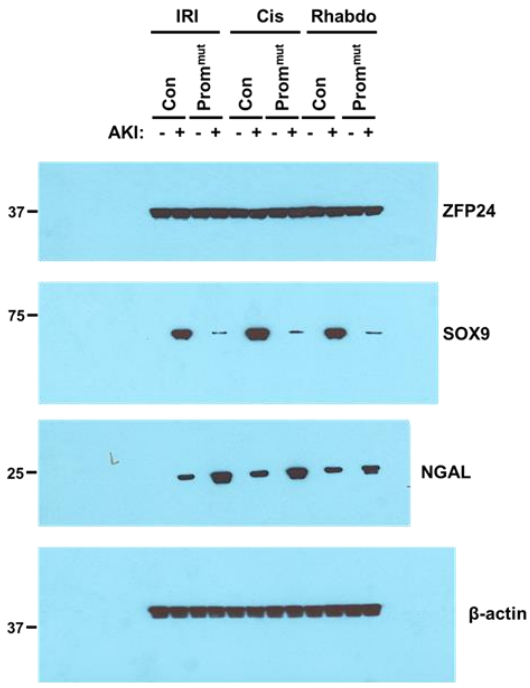

Figure 7c

Suppl. Figure S15: ***Uncropped images of immunoblot data.***

Supplementary Figure S15 (continued)

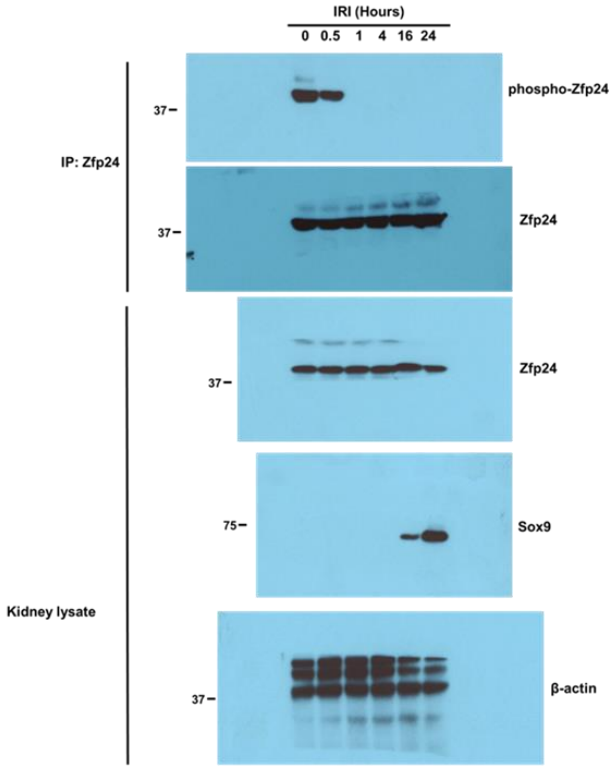

Supplementary Figure 3

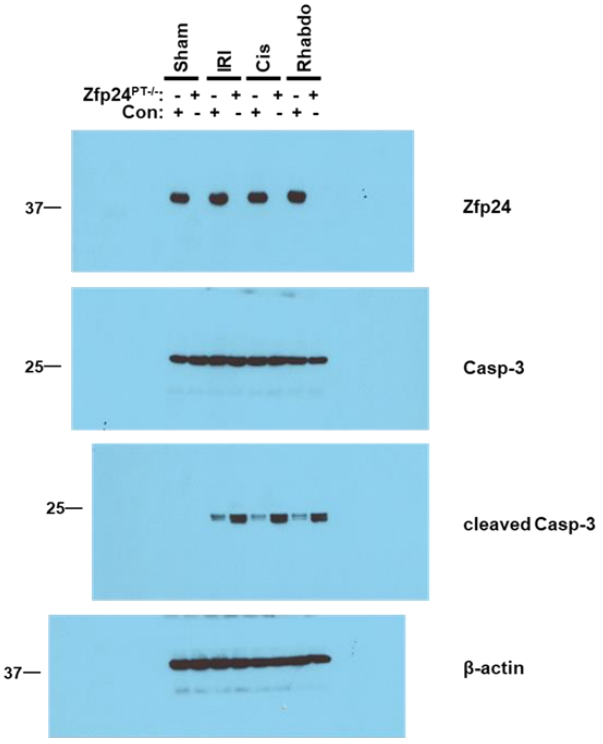

Supplementary Figure 5

Suppl. Figure S15: ***Uncropped images of immunoblot data.***

Supplementary Figure S15 (continued)

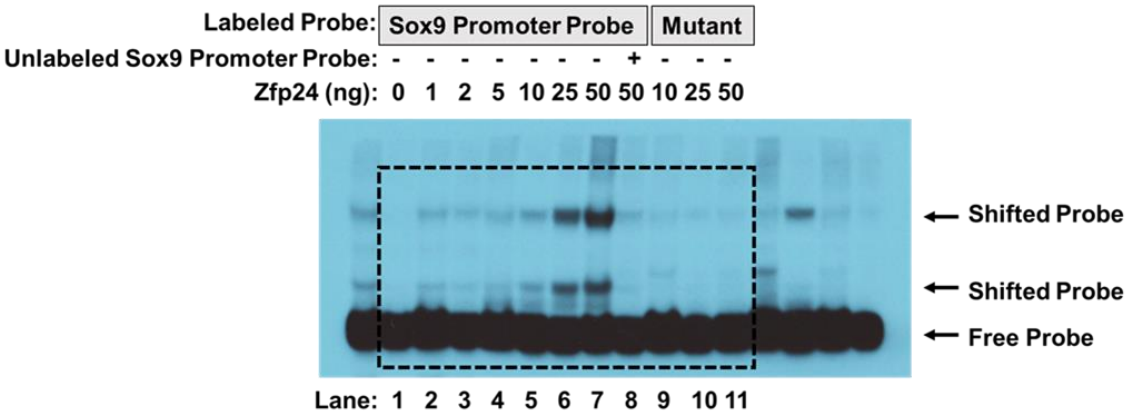

Supplementary Figure 10

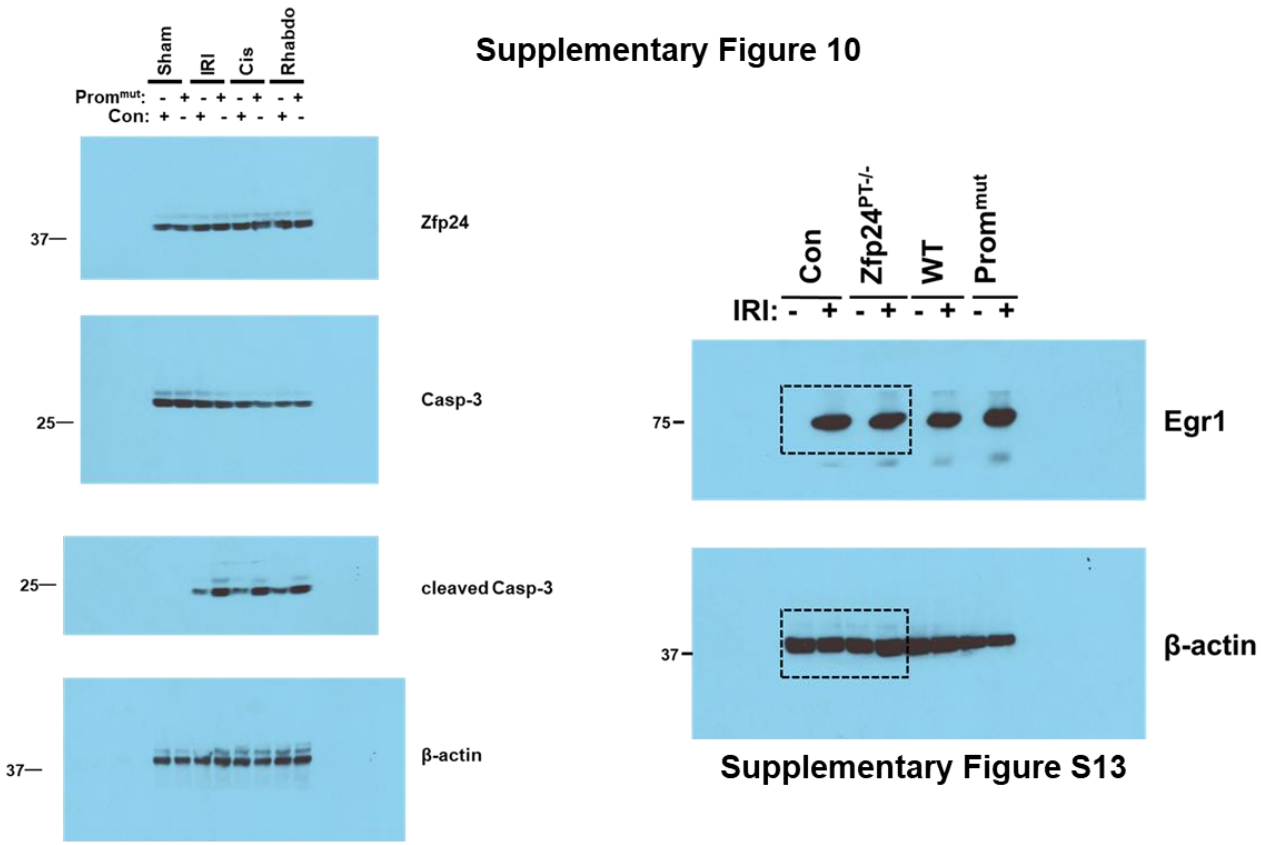

Supplementary Figure S13

Supplementary Figure S15

Suppl. Figure S15: ***Uncropped images of immunoblot data.***

Supplementary methods

Generation of Prom^{mut} mice. Knock-in mice with Zfp24 binding site mutation in the murine Sox9 promoter (-2017, TCAT to TAAT) were generated by standard methods at Applied StemCell (Milpitas, California). Briefly, Cas9 mRNA and gRNA were produced by in vitro transcription, oligo donor DNA was synthesized, and the mixture of Cas9 mRNA、 gRNA, and oligo DNA was microinjected into fertilized eggs (C57BL/6J). Two positive F0 mice were identified by PCR and DNA sequencing. The F0 mice were crossed with wild-type C57BL/6J mice to generate F1 mice, and then six positive F1 mice were identified by PCR and DNA sequencing. The heterozygous mice were then bred to generate wild-type and homozygous mutant littermates for further experiments. Mutations and genotypes were confirmed with DNA sequencing.

Assessment of kidney injury. Renal damage was assessed by serum analysis (blood urea nitrogen and creatinine) and histological examination (H&E staining). Mouse blood samples were collected at indicated time points, followed by blood urea nitrogen and creatinine measurement by QuantiChromTM Urea Assay Kit (DIUR-100) and enzymatic assay-based creatinine measurements (ab65340, Abcam). For histological analysis, mouse kidneys were harvested and embedded in paraffin at indicated time points before and after AKI induction. Tissue sections (4 μm) were stained with hematoxylin and eosin by standard methods. Histopathologic scoring was conducted in a blinded fashion by examining 10 consecutive 100× fields per section from at least three mice per group. Tubular damage was scored by calculation of the percentage of tubules that showed dilation, epithelium flattening, cast formation, loss of brush border and nuclei, and denudation of the basement membrane. The degree of tissue damage was scored based on the percentage of damaged tubules as previously described: 0, no damage; 1, <25%; 2, 25–50%; 3, 50–75%; and 4, >75%.

Immunoblot analysis. Renal cortical tissue were lysed in modified RIPA buffer [20 mM Tris·HCl (pH 7.5), 150 mM NaCl, 1 mM Na2EDTA, 1 mM EGTA, 1% Nonidet P-40, 2.5 mM sodium pyrophosphate, 1 mM β-glycerophosphate, protease, and phosphatase inhibitors] supplemented

with 1% SDS. Invitrogen bis-Tris gradient midigels were used for Western blot analysis, followed by detection by ECL reagent (Cell Signaling). Primary antibodies used for Western blot analysis were from Santa Cruz Biotechnology [β-actin (no. 47778) and NGAL (no. 50351)], Abcam [SOX9 (EPR14335-78) and Pro-Caspase-3 (ab32499)], R&D systems [Cleaved Caspase-3 (Asp175), MAB835], and Abbexa [ZNF24 (abx239672)]. All primary antibodies were used at 1:1,000 dilution. Secondary antibodies were from Jackson Immunoresearch and used at 1:2,000 dilutions. ImageJ was used for densitometric analysis.

Immunoprecipitation. To examine Zfp24 phosphorylation, immunoprecipitation experiments were performed using previously described methods[S1-S5]. Renal tissues were lysed with a buffer containing 150 mM NaCl, 1 mM EDTA, 1 mM EGTA, 1% (vol/vol) Triton X-100, 2.5 mM sodium pyrophosphate, 1 mM β-glycerol phosphate, 1 mM Na3VO4, 10 µg/ml leupeptin, 10 µg/ml aprotinin, 1 mM phenylmethylsulfonyl fluoride, 50 mM NaF, 0.2% (wt/vol) dodecyl β-d-maltoside, and 20 mM Tris (pH 7.5). The soluble extracts were then subjected to Zfp24 immunoprecipitation. Briefly, 500 µg of protein lysate was incubated with 2 µg of IgG or anti-Zfp24 antibody (Abbexa, abx239672) at 4 ^{o}C overnight, followed by the addition of 30 µl of agarose protein A/G beads. Bead-bound immunoprecipitates were washed and collected by centrifugation. Immunoprecipitates were then used for immunoblot analysis of total Zfp24 and phosphorylated Zfp24 using a phospho-linker antibody (Biolegend, 685702). The secondary antibody used for immunoblot analysis was from Abcam (VeriBlot for IP Detection Reagent, ab131366).

Gene expression analysis. Total RNA was extracted from renal tissues using the RNeasy Mini Kit (Qiagen), followed by assessment of RNA quality and quantity using NanoDrop. One microgram of total RNA was reverse transcribed using the high-capacity cDNA Reverse Transcription Kit (ThermoFisher Scientific), and quantitative PCR analysis was then performed using SYBR Green Master Mix with gene-specific pre-designed primers (Sigma). For quantitative analysis, target gene values were normalized to β-actin gene expression using the ΔΔCT value

method (where CT is threshold cycle). The primer sequences are provided in Supplementary Table S1.

Site-directed mutagenesis. The QuikChange II XL Site-Directed Mutagenesis Kit (Agilent Technologies) was utilized to generate promoter mutants, according to previously described methods[S4, S6, S7]. The QuikChange primer design program was used to design mutagenesis primers, and primers were synthesized by Integrated DNA Technologies. Mutant constructs were sequenced to confirm successful mutagenesis. The mutagenesis primer sequences are provided in Supplementary Table S1.

Chromatin immunoprecipitation (ChIP). ChIP assays were performed using the Pierce Magnetic ChIP Kit according to the manufacturer's instructions and our previous studies[S4, S6, S7]. Briefly, cross-linking with 1% formaldehyde was carried out in renal tissues, followed by quenching with glycine, harvesting, and DNA fragmentation by sonication. Precleared lysates were then incubated with 5 µg of anti-Zfp24 antibody (Abbexa, abx239672) overnight at 4 °C, followed by addition of Protein A + G magnetic beads and incubation for 4 h at 4 °C. Finally, the beads were collected and washed, and the protein–DNA complexes were eluted, cross-linking was reversed, and DNA purification was performed. Standard qPCR analysis was then carried out using primers spanning the Sox9 promoter. The primer sequences are provided in Supplementary Table S1.

Electrophoretic mobility shift assays (EMSA). The LightShift Chemiluminescent EMSA Kit (Thermo Scientific, 20148) was used according to established protocols. The principle for LightShift EMSA Detection is similar to immunoblot analysis. Briefly, the biotin 3’ end-labeled duplex DNA probe (Integrated DNA Technologies) was incubated with purified Zfp24 protein (Origene, TP505667) and electrophoresed on a native gel (non-denaturing 6% TBE-polyacrylamide gel, Novex, EC6265). The DNA was then transferred to a positive Biodyne B Nylon Membrane (Thermo Scientific, 77016), UV crosslinked, probed with streptavidin-HRP conjugate, and incubated with the substrate. A chemiluminescent nucleic acid detection module

Kit (Thermo Scientific, 89880) was used according to instructions provided in the manual and the blots were exposed to x-ray films for detection and visualization. A 50 bp probe surrounding the TCAT sequence in the Sox9 murine promoter was used in the assay. A mutant probe with TCAT to TAAT mutation was used as a control. The probe sequences are provided in Supplementary Table S1.

Primary murine tubular cell culture. Murine renal cortical tissues were minced and digested with 0.75 mg/ml collagenase IV (Thermo Fisher Scientific). The cells were centrifuged at 2000 × g for 10 min in DMEM/F-12 medium with 32% Percoll (Amersham Biosciences). After two washes with serum-free media, the cells were plated in collagen-coated dishes and cultured in DMEM/F-12 medium supplemented with 5 µg/ml transferrin, 5 µg/ml insulin, 0.05 µm hydrocortisone, and 50 µm vitamin C (Sigma-Aldrich). Fresh media was supplemented every alternate day, and after 5–7 days of growth, the isolated proximal tubular cells were trypsinized and replated at 1 × 105 cells/well in 24-well plates. To induce cell death, primary RTECs were incubated with 50 µm cisplatin (Sigma-Aldrich) in fresh culture medium for 24 h, followed by viability and caspase assays. At the end of the incubation period, cells from 24-well plates were harvested, followed by trypan blue staining and manual cell counting with a hemocytometer and/or by using the Countess Automated Cell Counter (Thermo Fisher Scientific); translucent cells were considered as viable and blue-stained cells were counted as dead. Cellular viability was calculated by dividing the number of viable cells by the total cell number, and each sample was done in triplicate. For caspase assays, the cells were lysed in a buffer containing 1% Triton X-100, and 10 µg of protein from cell lysates was added to an enzymatic assay buffer containing 50 µm DEVD-AFC for 60 min at 37 °C. Fluorescence at excitation 360 nm/emission 535 nm was measured, and free AFC was used to plot a standard curve. Subsequently, the standard curve was used to convert the fluorescence reading from the enzymatic reaction into the nm AFC liberated/mg protein/hour as a measure of caspase activity.

Supplementary References

S1. Wang J, Pabla N, Wang CY*, et al.* Caspase-mediated cleavage of ATM during cisplatin-induced tubular cell apoptosis: inactivation of its kinase activity toward p53. *Am J Physiol Renal Physiol* 2006; **291:** F1300-1307.

S2. Pabla N, Bhatt K, Dong Z. Checkpoint kinase 1 (Chk1)-short is a splice variant and endogenous inhibitor of Chk1 that regulates cell cycle and DNA damage checkpoints. *Proc Natl Acad Sci U S A* 2012; **109:** 197-202.

S3. Pabla N, Dong G, Jiang M*, et al.* Inhibition of PKCdelta reduces cisplatin-induced nephrotoxicity without blocking chemotherapeutic efficacy in mouse models of cancer. *J Clin Invest* 2011; **121:** 2709-2722.

S4. Kim JY, Bai Y, Jayne LA*, et al.* A kinome-wide screen identifies a CDKL5-SOX9 regulatory axis in epithelial cell death and kidney injury. *Nat Commun* 2020; **11:** 1924.

S5. Sprowl JA, Ong SS, Gibson AA*, et al.* A phosphotyrosine switch regulates organic cation transporters. *Nat Commun* 2016; **7:** 10880.

S6. Kim JY, Bai Y, Jayne LA*, et al.* SOX9 promotes stress-responsive transcription of VGF nerve growth factor inducible gene in renal tubular epithelial cells. *J Biol Chem* 2020; **295:** 16328-16341.

S7. van Oosterwijk JG, Buelow DR, Drenberg CD*, et al.* Hypoxia-induced upregulation of BMX kinase mediates therapeutic resistance in acute myeloid leukemia. *J Clin Invest* 2018; **128:** 369-380.

Supplementary Table S1

qPCR Primers	
Sox9	CTCATTACCATTTTGAGGGG
	AAAATACTCTGGTTGCAAGG
Myof	GGGAATTATAAACCCGGATAC
	ATCAAGAGAGGGAACAATCC
β-actin	GATGTATGAAGGCTTTGGTC
	TGTGCACTTTTATTGGTCTC
Vgf	CTTTGACACCCTTATCCAAGGCG
	GCTAATCCTTGCTGAAGCAGGC
Zfp24	GAGGACTTGGAGAGTGAGCTTG
	AGCATCCAGCTCAGAACTCGGT
Egr1	AGCGAACAACCCTATGAGCACC
	ATGGGAGGCAACCGAGTCGTTT
Mutagenesis Primers	
Mice Sox9 Promoter mutant (TCAT to TAAT)	ATATTTTATTAAGTATTTGTTCATTAATACATCCATTTATAAATATACCCTTAATACAAAATATGGAGAGA
	TCTCTCCATATTTTGTATTAAGGGTATATTTATAAATGGATGTATTAATGAACAAATACTTAATAAAATAT
Mice Sox9 Promoter mutant (TCAT to ACAT)	ATTTTATTAAGTATTTGTTCATGTATACATCCATTTATAAATATACCCTTAATACAAAATATGGAG
	CTCCATATTTTGTATTAAGGGTATATTTATAAATGGATGTATACATGAACAAATACTTAATAAAAT
Mice Sox9 Promoter mutant (TCAT to TCTT)	GCATTTTGAAATATTTTATTAAGTATTTGTTCAAGAATACATCCATTTATAAATATACCCTTAATAC
	GTATTAAGGGTATATTTATAAATGGATGTATTCTTGAACAAATACTTAATAAAATATTTCAAAATGC
Mice Sox9 Promoter mutant (TCAT to TCAA)	GGCATTTTGAAATATTTTATTAAGTATTTGTTCTTGAATACATCCATTTATAAATATACCCTTAATA
	TATTAAGGGTATATTTATAAATGGATGTATTCAAGAACAAATACTTAATAAAATATTTCAAAATGCC
Mice Sox9 Promoter deletion mutant (TCAT deletion)	GCATTTTGAAATATTTTATTAAGTATTTGTTCATACATCCATTTATAAATATACCCTTAATACAAAATATG
	CATATTTTGTATTAAGGGTATATTTATAAATGGATGTATGAACAAATACTTAATAAAATATTTCAAAATGC
Human Sox9 Promoter mutant (TCAT to TAAT)	TTTACATCTTCCTGAAAACTTATTAACAGGCGACTTAAAAATGGACT
	AGTCCATTTTTAAGTCGCCTGTTAATAAGTTTTCAGGAAGATGTAAA
ChIP qPCR Primers	
Sox9 Promoter	TGTCGCAGCACATTATATCTCTCCA
	GCAACGAAAACGACAGTGGCCT
EMSA Probes	
Sox9 promoter probe	GGTATATTTATAAATGGATGTATTCATGAACAAATACTTAATAAAATATTT
Sox9 Promoter mutant probe (TCAT to TAAT)	GGTATATTTATAAATGGATGTATTAATGAACAAATACTTAATAAAATATTT